

See discussions, stats, and author profiles for this publication at: <https://www.researchgate.net/publication/231660131>

Third-Harmonic Generation in Mixed-Valent Ru–Pyrazine Chains: A Theoretical Study

ARTICLE *in* THE JOURNAL OF PHYSICAL CHEMISTRY A · DECEMBER 1997

Impact Factor: 2.69 · DOI: 10.1021/jp9718313

CITATIONS

19

READS

12

3 AUTHORS, INCLUDING:



Alessandro Ferretti

Italian National Research Council

79 PUBLICATIONS 943 CITATIONS

SEE PROFILE



Giovanni Villani

Italian National Research Council

63 PUBLICATIONS 697 CITATIONS

SEE PROFILE

Third-Harmonic Generation in Mixed-Valent Ru–Pyrazine Chains: A Theoretical Study

Alessandro Ferretti, Alessandro Lami,* and Giovanni Villani

Istituto di Chimica Quantistica ed Energetica Molecolare del CNR, via Risorgimento 35, I-56126 Pisa, Italy

Received: June 4, 1997; In Final Form: August 4, 1997[®]

We present and discuss the results of a numerical investigation on the susceptibility for third-harmonic generation in mixed valent ruthenium–pyrazine chains (which we may call “Creutz–Taube chains”), whose skeleton is made by ruthenium ions bridged by pyrazine ligands. These compounds are described by a two-band Hubbard Hamiltonian, which, according to our previous results, is capable of reproducing the main features of the optical spectra in the near-IR–vis as a function of the total charge of the ion (i.e., the number of Ru^{2+} and Ru^{3+} ions). The third-harmonic susceptibility, computed exactly through a linear algebraic method (avoiding the sum over states) is remarkably high, suggesting that these compounds may be good candidates for nonlinear optics and photonics.

I. Introduction

The study of nonlinear optical properties of molecules and materials is recognized as a field of high scientific and technological interest. We briefly remind here the exciting possibilities offered by photonics in the field of signal-processing and computing. For example, a factor of 1000 is predicted for the improvement in the rate of telecommunications.^{1,2} The atomic and molecular physics also has benefited (and will further benefit) of the availability of high-frequency laser beams generated by a third-harmonic process. Much research work in this field is addressed toward the design and realization of organic materials,^{2–4} which should offer some advantages on the classical inorganic crystals, especially in two respects: better processability and quicker response time. The scientific community is also very active in the investigation of inorganic semiconductors, where the nonlinear properties may be enhanced by creation of quantum-confined nanostructures.^{5–6}

The role of theory in this field may be important, if it will reveal capable of furnishing not only computational tools, but also simple interpretative models which may serve as a guide when designing new materials or ameliorating the existing ones, for example by introducing suitable substituents (tailoring). The most interesting development in this respect is the interpretation of nonlinear properties of a molecules in terms of a set of anharmonic oscillators,⁷ of electronic origin. The idea is old, and may be considered as a generalization of the Lorentz idea.⁸ Very recently it has been popularized by Mukamel and co-workers,^{9–11} who connected it to the time-dependent Hartree–Fock approach (RPA). In these papers the oscillators are identified by analyzing the time-dependent one-particle density matrix. The above methodology, unfortunately, seems to be not applicable to strongly correlated electron systems, being founded on the hypothesis that the system can be described by a single (time-dependent) Slater determinant at all times. In studying these systems one must resort to new methods.

In this paper we examine a class of such compounds, i.e., the mixed valent chains of ruthenium ions bridged by pyrazine units (Figure 1), whose prototype is the well-known Creutz–Taube ion.¹² Some of these compounds have been prepared and studied several years ago, as far as the optical absorption spectra are concerned.¹³ Recently, we proposed a simple model for these compounds, which revealed very useful in reproducing

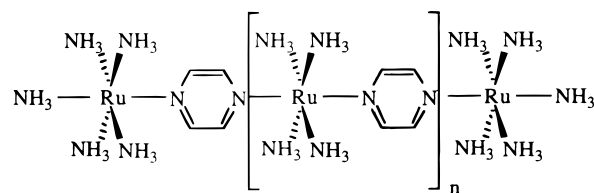


Figure 1. Ru–pyz chains.

and interpreting the change of the near-IR–vis optical properties when the total charge of the ion is varied.^{14–17} Here we study the same compounds from the point of view of nonlinear optical properties. The plan of the paper is the following: in the next section we briefly review the main optical properties of such compounds and the model proposed for their study; in section II we present the method we have adopted for the computation of nonlinear optical properties, which may be considered a linear algebraic version of the inhomogeneous differential equation method, proposed several years ago by Dalgarno and Lewis,¹⁸ for computing the action of the resolvent operator on a given state, avoiding the sum-over-states representation; in Section III we present and discuss some numerical results for our chain compounds, while the meaning of the work is resumed in a few concluding remarks.

II. Creutz–Taube Chains

The Creutz–Taube ion is a well-known mixed-valence system built by two ruthenium ions, each one coordinated to five ammonia molecule, with a pyrazine molecule bridging the two $\text{Ru}(\text{NH}_3)_5$ moieties. The interesting optical properties of such compound depends on the back-bonding from the ruthenium ion to the π^* orbital of the pyrazine. Due to distorted symmetry, the electron transfer processes may be simply modeled by just taking one orbital per center: a d_{xz} orbital on each ruthenium and the LUMO (π^*) on the pyrazine (taking the Ru–Ru axis as x and the axis perpendicular to the pyrazine plane as z). The Ru^{3+} has a d^5 configuration, and hence, it has one electron in the d_{xz} orbitals, which is pushed toward higher energy by the distorted octahedral field.¹⁹ The species $\text{Ru}(\text{III})$ – $\text{Ru}(\text{III})$, $\text{Ru}(\text{III})$ – $\text{Ru}(\text{II})$ and $\text{Ru}(\text{II})$ – $\text{Ru}(\text{II})$ have then two, three, and four electrons, respectively. In previous studies we have shown that the spectral behavior of all the above species, as well as their longer analogues, is remarkably well reproduced by the two-

[®] Abstract published in *Advance ACS Abstracts*, November 15, 1997.

band Hubbard Hamiltonian:

$$H_{\text{mol}} = E_{\text{Ru}}(n_1 + n_3 + \dots + n_N) + E_{\text{pyz}}(n_2 + n_4 + \dots + n_{N-1}) + t \sum_{\sigma} [(a_{1,\sigma}^+ a_{2,\sigma} + a_{2,\sigma}^+ a_{3,\sigma} + \dots + a_{N-1,\sigma}^+ a_{N,\sigma}) + h.c.] + U(n_{1\uparrow} n_{1\downarrow} + n_{3\uparrow} n_{3\downarrow} + \dots + n_{N\uparrow} n_{N\downarrow}) \quad (1)$$

where

$$n_j = n_{j\uparrow} + n_{j\downarrow}$$

The following values of the parameters will be considered, which have been optimized to reproduce the absorption spectra of the Creutz–Taube ion and its monovalent analogues: $t = -0.73$, $U = 4.62$, and $\Delta = E_{\text{pyz}} - E_{\text{Ru}} = 5.06$ (all in eV).

According to our interpretation, the peculiar properties of such compounds depend on the fact that, despite the large bandgap Δ , the hopping from a doubly occupied Ru orbital to the pyrazine is easy, owing to the strong electron–electron repulsion on the ruthenium sites (U). The near-infrared intervalence transition in the mixed valent Ru(III)–Ru(II) complex is attributed to a transition from the symmetric ground state to an antisymmetric excited state, without appreciable variation in the charge distribution.

The same model Hamiltonian of eq 1 rationalizes the behavior of the longer chain analogues of the Creutz–Taube ion, first synthesized and studied by Von Kameke, Tom and Taube¹³ (up to 5 ruthenium ions bridged by four pyrazine units). The number of electrons in the system can be easily changed by adding an oxidant and the corresponding absorption spectra are found to vary.¹³ The most impressive feature of these spectra is that, as one begins to remove electrons from the fully reduced species (i.e., that with all Ru(II)), a transfer of spectral weight from higher to lower frequencies is observed. This persists until the number of Ru(III) and Ru(II) is balanced^{15,16} (the computed spectra are reported in the section III, when discussing nonlinear optical behavior). This situation is reminiscent of what observed in high T_c copper-oxide superconductors, when doping with holes.^{20,21}

According to our model, the above behavior may be interpreted as a pronounced increase in the electron mobility, when one has an almost alternance between Ru(III) and Ru(II) along the chain. The ground state of the system exhibits then strong charge fluctuations between Ru and pyrazine sites.¹⁵ Again, the reason may be found in the fact that the U term almost compensates the energy gap between the d_{xz} orbital and the LUMO of the bridging ligand. The presence of an absorption band at low frequency (below 0.5 eV), not reported in the experimental results of ref 13, for chains with 5 ruthenium ions and the overall tendency toward lower frequencies by increasing the dimensions of the system strongly support the idea that longer chains (if they can be prepared) may behave as small-gap semiconductors or even metals. In this paper, however, we focus on the nonlinear optical properties of chains, as can be exactly computed within our Hubbard model of eq 1.

III. Linear Algebraic Method for the Computation of Linear and Nonlinear Optical Properties

When a molecule is placed in an external e.m. field it may give rise to a number of processes involving photon absorption and emission. If we do not investigate on processes induced by very short pulses, it is convenient to work in a time-independent formalism, taking into account the radiation Hamil-

tonian as well as the molecule-field interaction in the second quantization formalism. Neglecting the spatial dependence of the field in the spirit of the dipole approximation, as well as magnetic interactions, the full Hamiltonian is then written as

$$H = H_{\text{mol}} + H_{\text{rad}} + V$$

$$H_{\text{rad}} = \sum_{k,\lambda} \omega_k b_k^+(\lambda) b_k(\lambda)$$

$$V = -\mu E \quad (2)$$

where k is the wave vector of the photon, λ its polarization, μ is the molecular dipole, and E the electric field (which can be written in terms of photon creation–annihilation operators).

As is well-known, the probability of a given process, identified by the initial and final state (both including photons) can then be evaluated from the matrix element of the scattering operator T :^{22,23}

$$P_{f \leftarrow i} = |\langle f | T | i \rangle|^2 \rho_f \quad (3)$$

where ρ_f is the density of final states for the process.

Processes involving a given number of photon absorption–emission can be extracted from eq 3 through the expansion^{22,23}

$$T = V + VG_0V + VG_0VG_0V + \dots$$

where

$$G_0 = \frac{1}{E_f - H_{\text{mol}} - H_{\text{rad}}} \quad (4)$$

Our interest in this paper is for coherent harmonic generation processes, in which a certain number of photons is absorbed from the initially populated radiation mode and spontaneously emitted in an empty mode with double, triple, ... frequency.

Due to the vector nature of both molecular dipole and electric field, the matrix elements of \mathbf{T} for n -harmonic generation can be formally written as a $n + 1$ tensor contraction of two distinct tensor factors, one for the molecule (the susceptibility) and the other for photons.²² In the present case the transition dipole matrix elements are all aligned along the x -axis (the Ru–Ru axis) and we can then simplify our notation, focusing on the molecular part.

The various susceptibilities may be written in the usual form of a sum over states by introducing in eq 4 the spectral representation of the unperturbed resolvent operator. The susceptibility involved in the second-harmonic generation is then the following sum of three terms, corresponding to the diagrams a–c in Figure 2:

$$\chi_2(-2\omega; \omega, \omega) = \frac{1}{2} \sum_{j,k} \left[\frac{\langle g | \mu | k \rangle \langle k | \mu | j \rangle \langle j | \mu | g \rangle}{(\Delta_{gk} + 2\omega + i\gamma_k)(\Delta_{gj} + \omega + i\gamma_j)} + \frac{\langle g | \mu | k \rangle \langle k | \mu | j \rangle \langle j | \mu | g \rangle}{(\Delta_{gk} - \omega - i\gamma_k)(\Delta_{gj} + \omega + i\gamma_j)} + \frac{\langle g | \mu | k \rangle \langle k | \mu | j \rangle \langle j | \mu | g \rangle}{(\Delta_{gk} - \omega - i\gamma_k)(\Delta_{gj} - 2\omega - i\gamma_j)} \right] \quad (5)$$

In eq 5 $\Delta_{gj} = E_g - E_j$ etc. According to the usual rules the line width γ of excited states is taken positive for virtual steps.²⁴ The numerical factor 1/2 is introduced here for homogeneity with the Orr–Ward result²⁵ (see also ref 4). For the chains discussed in section II χ_2 is identically zero since the molecule is centrosymmetric.

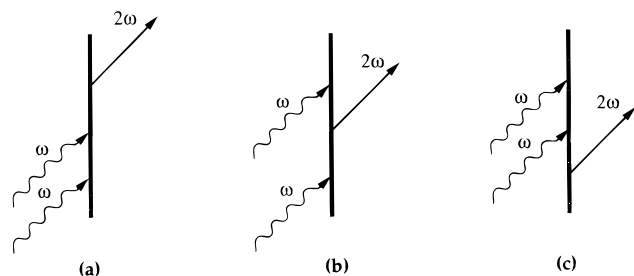


Figure 2. Three Feynmann diagrams for the processes contributing to second-harmonic generation. On the left side of the thick vertical line are the absorptions of photons ω , on the right the emission of a photon 2ω .

The susceptibility involved in the third-harmonic generation is the following sum of four terms, corresponding to the diagrams a–d in Figure 3:

$$\chi_3(-3\omega; \omega, \omega, \omega) = \frac{1}{4} \sum_{j,k,l} \left[\frac{\langle g|\mu|l\rangle\langle l|\mu|k\rangle\langle k|\mu|j\rangle\langle j|\mu|g\rangle}{(\Delta_{gl} + 3\omega + i\gamma_l)(\Delta_{lk} + 2\omega + i\gamma_k)(\Delta_{gj} + \omega + i\gamma_j)} + \frac{\langle g|\mu|l\rangle\langle l|\mu|k\rangle\langle k|\mu|j\rangle\langle j|\mu|g\rangle}{(\Delta_{gl} - \omega - i\gamma_l)(\Delta_{lk} + 2\omega + i\gamma_k)(\Delta_{gj} + \omega + i\gamma_j)} + \frac{\langle g|\mu|l\rangle\langle l|\mu|k\rangle\langle k|\mu|j\rangle\langle j|\mu|g\rangle}{(\Delta_{gl} - \omega - i\gamma_l)(\Delta_{lk} - 2\omega - i\gamma_k)(\Delta_{gj} + \omega + i\gamma_j)} + \frac{\langle g|\mu|l\rangle\langle l|\mu|k\rangle\langle k|\mu|j\rangle\langle j|\mu|g\rangle}{(\Delta_{gl} - \omega - i\gamma_l)(\Delta_{lk} - 2\omega - i\gamma_k)(\Delta_{gj} - 3\omega - i\gamma_j)} \right] \quad (6)$$

The numerical factor 1/4 is introduced here for the same reasons mentioned in the case of second-harmonic generation.

We also notice that absorption processes may be treated within the same formalism, utilizing the optical theorem.²⁶ The absorption cross section is related to the imaginary part of the amplitude for the elastic processes (initial and final states identical for both molecule and photons). Using the expansion of \mathbf{T} one may distinguish between single-photon, $A_1(\omega)$, two-photon, $A_2(\omega)$, ..., absorption spectra:

$$A_1(\omega) \propto -\text{Im} \sum_j \frac{|\langle g|\mu|j\rangle|^2}{\Delta_{gj} + \omega + i\gamma_j} \quad (7a)$$

$$A_2(\omega) \propto -\text{Im} \sum_{j,k,l} \frac{\langle g|\mu|l\rangle\langle l|\mu|k\rangle\langle k|\mu|j\rangle\langle j|\mu|g\rangle}{(\Delta_{gl} + \omega + i\gamma_l)(\Delta_{lk} + 2\omega + i\gamma_k)(\Delta_{gj} + \omega + i\gamma_j)} \quad (7b)$$

The sum-over-states representation of susceptibility tensors has the advantage of showing explicitly the contributions coming from the various electronic states but, in principle, is amenable to numerical calculation only if a good representation of the whole set of excited states is at hand. Despite this intrinsic limitations the sum-over-states method has been extensively used.^{2,4} We have successfully tested a different approach, which is basically an algebraic version of the one proposed by Dalgarno and Lewis¹⁸ and used successfully for computing multiphoton amplitudes.²³ A very similar method has been applied by Soos and Ramasesha²⁷ to the study of nonlinear properties of conjugated system by their diagrammatic valence bond theory.

For illustrating the method let us first consider the resonant polarizability term:

$$\chi_1^+(\omega) = \langle d|a\rangle \quad (8)$$

where

$$|d\rangle = \mu|g\rangle$$

$$|a\rangle = G_0(E_g + \omega + i\gamma)|d\rangle \quad (9)$$

Here, for simplicity, we have taken the same damping factor for all the excited states. The ground state is obtained by a Lanczos approach (see ref 14–16 for more details) and we can also easily generate the doorway state $|d\rangle$, eq 9, since the dipole operator is diagonal in our localized (valence bond) basis set.¹⁷ The computational problems arise for computing the vector $|a\rangle$, eq 9, since in order to evaluate G_0 one has to invert a large matrix. The problem can be overcome rewriting eq 9 in the form:

$$|d\rangle = (E_g + \omega - H_0 + i\gamma)|a\rangle \quad (10)$$

and $|a\rangle$ can be found solving an inhomogeneous system of linear equations, whose dimension is that of the basis set. We notice that if, as in the Dalgarno–Lewis method, H_0 is a differential operator instead of a matrix, one is lead to an inhomogeneous differential equation.^{12,23} The doorway state $|d\rangle$ is real, but we take it as complex for generality (in fact, as we will see, for the calculation of higher order polarizabilities one has to solve an eq like (10) in which both $|a\rangle$ and $|d\rangle$ have to be replaced by new complex vectors having a different meaning):

$$|a\rangle = |x\rangle + i|y\rangle$$

$$|d\rangle = |u\rangle + i|w\rangle \quad (11)$$

We solve the above linear system by an iterative method searching, for each frequency ω , the minimum of the function (N is the dimension of the basis set):

$$f(x_1, x_2, \dots, x_n, y_1, y_2, \dots, y_n) = \sum_j \{[(E_g + \omega - H_0)x_j - u_j]^2 + (\gamma y_j - w_j)^2\} \quad (12)$$

where x_j is the j th component of the vector $|x\rangle$ along the basis set, etc. The point at which the function f reaches its minimum value gives the required vector $|a\rangle$. As is well-known, since the above is a quadratic function, one could trivially find the minimum by solving a linear system involving the gradient vector and the Hessian matrix.²⁷ The direct approach, however, cannot be pursued when N is very large, since it requires the inversion of the Hessian matrix. One is then forced to minimization methods that utilize only the gradient vector. We have tested the conjugate gradient method by Fletcher and Reeves²⁸ and have found that it works very well. In the Appendix we give the explicit form of the gradient vector, which is the basic ingredient of the method. Here we simply remind that iterative methods work speedily on large systems if the vector produced by acting with H_0 on $|a\rangle$ is easily generated, without having to store the whole H_0 matrix. This is our case, due to the sparse nature of the matrix representation of the model Hamiltonian in eq 1.

It is also clear that the method can be easily generalized to higher order susceptibility. This can be done in two distinct ways: (1) by a sequential procedure; (2) by a single step procedure. Let us illustrate this for the first term, $\chi_3^{(1)}$, of the

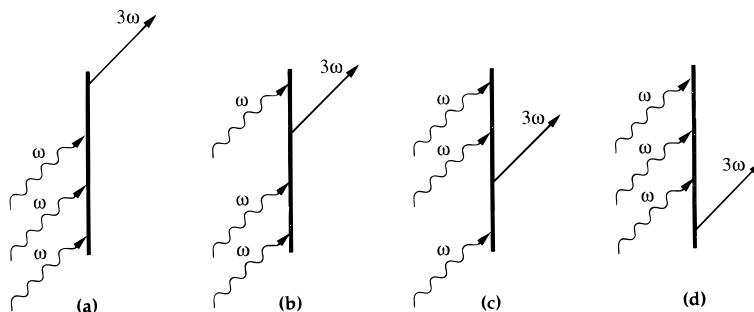


Figure 3. Four Feynmann diagrams for the processes contributing to third-harmonic generation. On the left side of the thick vertical line are the absorptions of photons ω , on the right the emission of a photon 3ω .

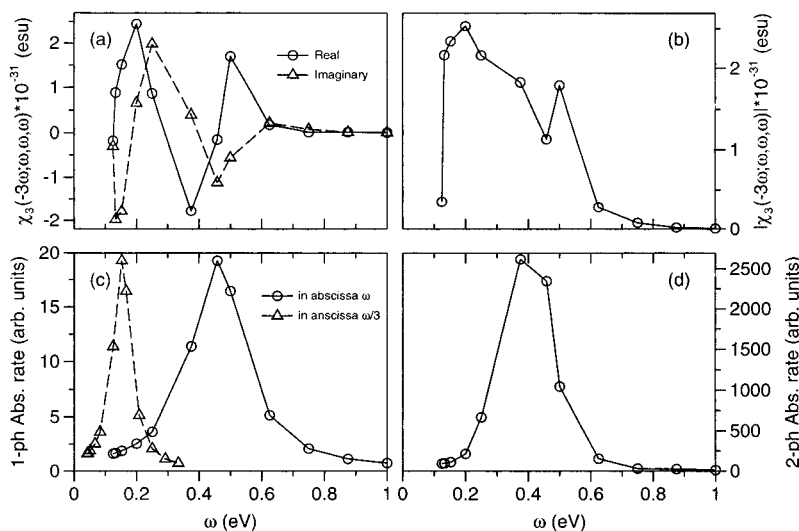


Figure 4. Various computational results obtained for the seven sites, six electrons chain: (a) real and the imaginary part of $\chi_3(-3\omega; \omega, \omega, \omega)$; (b) absolute value of χ_3 ; (c) one-photon absorption rate as a function of ω (continuous line) and of $\omega/3$ (broken line) (see text); (d) two-photon absorption rate. For the absorption rate curves we simply report the value of the sums in eqs 7a and 7b. To obtain the rate in number of transitions per atomic unit of time, the ordinates in Figure 3c have to be multiplied by the factor $2\pi d^2 p(\rho/2)^2$, where ρ is the energy density in au (number of photons times photon energy divided by quantization volume), d is the distance between sites (in au) and $p = 27.2114$ is the au-eV conversion factor. The ordinates in Figure 3d have to be multiplied by $2\pi d^3 p(\rho/2)$.⁴ In computing parts a and b of Figure 3, we have assumed $d = 2 \text{ \AA}$.

susceptibility tensor involved in second harmonic generation, eq 2. (1) One starts from $|d\rangle$ to determine $|a\rangle$ as illustrated previously for the polarizability; $|d'\rangle = \mu|a\rangle$ is then easily generated. The vector $|d'\rangle$ is used to determine

$$|a'\rangle = G_0(E_g + 2\omega + i\gamma)|d'\rangle$$

by the same iterative method. Finally,

$$\chi_2^{(1)}(-2\omega; \omega, \omega) = \langle d|\mu|a'\rangle$$

(2) After defining $|a'\rangle = F|d\rangle$ with

$$F = G_0(E_g + 2\omega + i\gamma)\mu G_0(E_g + \omega + i\gamma)|d\rangle$$

one can directly go to the linear system

$$F^{-1}|a'\rangle = (E_g + 2\omega + i\gamma)\mu^{-1}(E_g + \omega + i\gamma)|a'\rangle = |d\rangle$$

since the dipole operator is diagonal and can be easily inverted. We have used the first route for our calculation of third harmonic generation in Creutz-Taube chains, since it offers the advantage that the intermediate results can be also used to compute two-photon absorption spectra.

IV. Numerical Results and Discussion

We have computed the third-harmonic susceptibility tensor for chains involving 7 and 9 sites, i.e., four ruthenium ions bridged

by three pyrazine molecules and five ruthenium ions bridged by four pyrazine molecules, respectively. As far as the oxidation state is concerned, we have selected two cases in which the transfer of spectral weight to low frequency is higher. As previously mentioned this happens when the number of ruthenium ions with oxidation state +3 and +2 is identical, when possible (for seven sites). For nine sites we have taken three Ru^{3+} ions and two Ru^{2+} ions (we remember that, due to the strong electron delocalization in such complexes, the assignment of +2 and +3 charges is arbitrary and has been introduced just for counting electrons). Since our model, as previously mentioned, takes into account only electrons involved in the back-bonding from the d_{zx} atomic orbital on each Ru atom to the π^* molecular orbital of each pyrazine molecule (LUMO), we have included in the calculation six electrons (for seven sites) and seven electrons (nine sites). The number of Slater determinants in our computation (selecting those with the minimum total S_z) is then 1225 (for the seven sites, six electrons case) and 10 584 (nine sites and seven electrons).

In Figure 4 we show, for the seven sites, six electrons chain, as a function of (in the range 0–1 eV): (a) the real and imaginary part of $\chi_3(-3\omega; \omega, \omega, \omega)$, (b) its absolute value. The damping term γ , the same for all the excited states, has been taken to be 0.1 eV. To elucidate the contributions coming from intermediate resonant steps due to states which can be reached by absorption of one, two or three photons, we reported on the same figure the single-photon, and the two-photon absorption

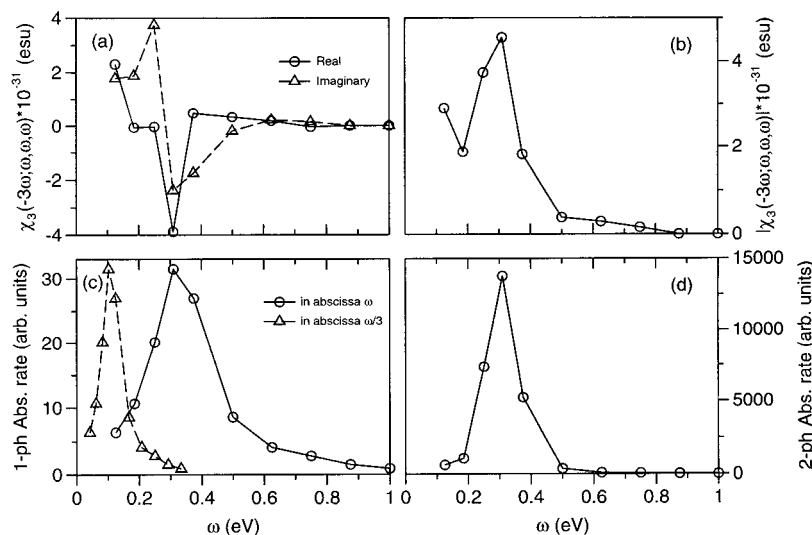


Figure 5. Same as in Figure 3 for the nine sites, seven electrons chain.

spectrum (Figure 4c and 4d, respectively). We have not computed the three-photon absorption spectrum. Some information on the effect of the three-photon resonances may be extracted looking at the one-photon absorption spectrum as a function of $\omega/3$ (dashed line in Figure 4c), due to the fact that the states that can be reached by one- and three-photon absorption are the same. Similar information can be extracted from the real and the imaginary part of $\chi_3(-3\omega; \omega, \omega, \omega)$, reported in Figure 4a. The parametric (nonresonant) generation is larger for values of ω at which the real part of $\chi_3(-3\omega; \omega, \omega, \omega)$ dominates.

Figure 5 has the same content of Figure 4, but refers to the nine sites, seven electrons chain.

The first remark suggested from a perusal of Figures 4 and 5 is that the computed susceptibility values are very high, as one may realize comparing them with the known experimental values for various materials.^{3,4,10} For example, the polyacetylene has values of $\chi_3(-3\omega; \omega, \omega, \omega)$ of the same order of magnitude of those of the seven sites, six electrons Creutz-Taube chain (Figure 4), while in the nine sites, seven electrons chain χ_3 (Figure 5) further increases by a factor of about 2. The high values obtained depend on the large transition moments involved (along the chain axis), permitted by the peculiar electronic structure of such compounds, as it results from our calculations. The latter, is deeply influenced by the strong correlation effects on the metallic sites, and by the fact that all the Ru-pyz distances along the chain have been assumed identical, in contrast with the strong bond alternation present in polyenes. Our assumption is supported by the experimental observation that the Ru-pyz distance is almost the same for Ru(II) and Ru(III) complexes^{29,30} but need to be confirmed by direct experimental observation in the chains (we were not able to find experimental data in the literature).

Comparing part b with parts c and d of Figure 4 (seven sites, six electrons), one may assign the two peaks in the absolute value of the third-order susceptibility (Figure 4b) to the resonant absorption of one photon (right peak) and three photons (left peak). The two-photon absorption spectrum has a single peak at a frequency value very close to that for the single photon absorption, reflecting the fact that the two-photon absorption is also enhanced by the one-photon resonance. As a consequence, is not easy to extract a definite conclusion on the role of two-photon resonance(s).

The behavior in Figure 5 (nine sites, seven electrons) is similar. Here, the peak at about 0.3 eV (Figure 5b) is almost coincident with a one-photon resonance (Figure 5c) and a peak

in the two-photon absorption spectrum (Figure 5c). Once again, is not clear if there is a specific role of two-photon resonances. The peak at low frequency may be related to a three-photon resonance.

Direct information on the role of resonant and nonresonant processes may be obtained from Figures 4a and 5a, showing the real and imaginary part of the third-order susceptibility for third harmonic generation. The frequency ranges at which the real part of χ_3 dominates are those at which one expects parametric amplification.

As a general remark, we notice that according to our computations, the contributions coming from diagrams involving virtual steps, parts b–d of Figure 3, are also very important and cannot be neglected.

V. Conclusions

Our work shows that the third-harmonic generation process seems to proceed with high probability in the mixed valence Creutz-Taube chains, i.e., ruthenium ions bridged by pyrazine ligands (the coordination environment is saturated by ammonia molecules to give an almost octahedral geometry) studied several years ago by Von Kameke et al.¹³ This is not unexpected for us, since previous calculations with the same Hubbard model Hamiltonian used here (but slightly different parameters) showed remarkable static charge fluctuations along the chain, in the ground state.¹⁵ What we find here is that these oscillations are dynamically amplified by the e.m. field and they exhibit a strong nonlinear behavior. The computed microscopic χ_3 for the chain with seven sites (four Ru atoms and three pyz bridges) and six electrons has the same order of magnitude of that in polyacetylene, while moving to the nine sites, seven electrons chain it further increases by a factor of about 2. We have presented here some preliminary results obtained by a numerical method avoiding the sum-over-states bottleneck in the spirit of the Dalgarno-Lewis approach.^{18,23} The method shares many similarities with that proposed by Soos and Ramasesha.²⁷ We are currently extending the calculations to cover different number of electrons and chain lengths. We are also planning to investigate the role of electron-phonon interaction on the nonlinear optical behavior of such compounds. The analysis of results will furnish new elements for a physical interpretation of the nonlinear properties of such mixed-valent chains. We will be very happy if, meanwhile, some experimental results on these chains, hopefully stimulated by the present paper, will

also appear to enrich the literature, which, to our knowledge, is very scarce on this particular argument.

Appendix

We give here an explicit expression for the gradient of eq 12. This refers to the resonant term of the first polarizability, but it may be easily generalizable to all the terms we need (in general instead of ω we may have $n\omega$ where n may be negative and γ has to be taken negative in some cases, see eqs 5 and 6).

Let us first rewrite eq 12 making explicit the first term in the sum on the right side:

$$f(x_1, x_2, \dots, x_N, y_1, y_2, \dots, y_N) = \sum_j \{ [\sum_k ((E_g + \omega)\delta_{jk} - H_{0jk})x_k - u_j]^2 + (\gamma y_j - w_j)^2 \}$$

The gradient (row) vector has then the following components along x_i and y_i , respectively:

$$(\nabla f)_x = p[(E_g + \omega)\mathbf{I} - H_0]$$

$$(\nabla f)_y = 2\gamma[\gamma y - w]^T$$

where

$$p = 2(r - \tilde{u})[(E_g + \omega)\mathbf{I} - H_0]$$

$$r = \{[(E_g + \omega)\mathbf{I} - H_0]x\}^T$$

Here, \mathbf{I} is the $N \times N$ identity matrix and a right-side upper T indicates the transpose.

Acknowledgment. The authors acknowledge their participation in the MITER National Institute of CNR (Materiali Speciali e Tecnologie Relative).

References and Notes

- (1) Hinton, H. S. *IEEE Spectrum* **1992**, February, 42.

- (2) Bredas, J. L.; Adant, G.; Tackx, P.; Persons, A. *Chem. Rev.* **1994**, 94, 243.
- (3) Prasad, P. N. *Chem. Mater.* **1990**, 2, 660.
- (4) Prasad, P. N.; Williams, D. J. *Introduction to Nonlinear Optical Effects in Molecules & Polymers*; John Wiley & Sons: New York, 1991.
- (5) Brus, L. *IEEE J. Quantum Electron.* **1986**, QE22, 1909.
- (6) Flytzanis, C. In *Materials for Photonic Devices*, D'Andrea, A., Lapicciarella, A., Marletta, G., Viticoli, S., Eds.; World Scientific: Singapore, 1991; p 359.
- (7) Bloembergen, N. *Nonlinear Optics*; Benjamin: New York, 1965.
- (8) Fano, U. *Rev. Mod. Phys.* **1957**, 29, 74.
- (9) Wang, H. X.; Mukamel, S. *J. Chem. Phys.* **1992**, 97, 8019.
- (10) Takahashi, A.; Mukamel, S. *J. Chem. Phys.* **1991**, 100, 2366.
- (11) Chen, G.; Mukamel, S. *J. Am. Chem. Soc.* **1995**, 117, 4945.
- (12) Creutz, C.; Taube, H. *J. Am. Chem. Soc.* **1973**, 95, 1086.
- (13) Von Kameke, A.; Tom, G. M.; Taube, H. *Inorg. Chem.* **1978**, 17, 1790.
- (14) Ferretti, A.; Lami, A. *Chem. Phys.* **1994**, 181, 107.
- (15) Ferretti, A.; Lami, A. *Chem. Phys.* **1994**, 186, 143.
- (16) Ferretti, A.; Lami, A. *Chem. Phys. Lett.* **1994**, 220, 327.
- (17) Ferretti, A.; Lami, A.; Villani, G. submitted to *Inorg. Chem.*
- (18) Dalgarno, A.; Lewis, J. J. *Proc. Phys. Soc. A* **1955**, 233, 70.
- (19) Neunschwander, N.; Piepho, S. B.; Wong, K. J.; Day, P. *J. Am. Chem. Soc.* **1985**, 107, 7862.
- (20) Cooper, S. L.; Thomas, G. A.; Orenstein, J.; Rapkine, D. H.; Capizzi, M.; Timusk, T.; Millis, A. J.; Schneemeyer, L. F.; Waszczak, J. W. *Phys. Rev. B* **1989**, 40, 11358.
- (21) Uchida, S.; Ido, T.; Takagi, H.; Arima, T.; Tokura, Y.; Tajima, S. *Phys. Rev. B* **1991**, 43, 7942.
- (22) Andrews, D. L. In *Modern Nonlinear Optics*, Part 2; Edited by Evans, M., and Kielich, S.; Advances in Chemical Physics Series, Vol LXXXV; p 545.
- (23) Faisal, F. H. M. *Theory of Multiphoton Processes*; Plenum Press: New York, 1987.
- (24) Hanna, D. C.; Yuratich, M. A.; Cotter, D. *Nonlinear Optics of Free Atoms and Molecules*; Springer, Berlin, 1979.
- (25) Orr, B. J.; Ward, J. F. *Molecular Phys.* **1971**, 20, 513.
- (26) Taylor, J. R. *Scattering Theory*; John Wiley & Sons: New York, 1972.
- (27) Soos, S. G.; Ramasesha, S. *J. Chem. Phys.* **1989**, 90, 1057.
- (28) Fletcher, R. *Practical Methods of Optimization*; John Wiley & Sons: New York, 1980; Vol. 1.
- (29) Fürholz, U.; Bürgi, H. B.; Wagner, F. E.; Stebler, A.; Ammeter, J. H.; Krausz, E.; Clark, R. J. H.; Stead, M. J.; Ludi, A. *J. Am. Chem. Soc.* **1984**, 106, 121.
- (30) Ondrechen, M. J.; Gozashiti, Wu, X. M. *J. Chem. Phys.* **1992**, 96, 3255.